

# Optimisation of the Q Factor of a Complementary Frequency Selective Surface

C.K. Lee<sup>1</sup>, S.S. Bukhari<sup>2</sup>, J.(Yiannis) C. Vardaxoglou<sup>3</sup> and W.G. Whittow<sup>4</sup>

<sup>1,2,3,4</sup>Wolfson School of Mechanical, Electrical and Manufacturing Engineering,  
Loughborough University, LE11 3TU, Leicestershire, UK

<sup>1</sup>C.Lee2@lboro.ac.uk, <sup>2</sup>S.S.Bukhari@lboro.ac.uk, <sup>3</sup>J.C.Vardaxoglou@lboro.ac.uk, <sup>4</sup>W.G.Whittow@lboro.ac.uk

**Keywords:** complementary frequency selective surface; Q factor; metasurface

## Abstract

The complementary frequency selective surface (CFSS) consists of an array of dipoles and slots either side of a thin dielectric and exhibits a sharp passband. The conductors layer adds capacitance to the apertures layer which in turn miniaturises the FSS. In this paper, the CFSS is placed in a waveguide and the Q factor is maximised by varying the electric properties and physical parameters. The fabricated CFSS structure shows good agreement with the simulations.

## 1 Introduction

Frequency selective surfaces (FSS) have been studied for many years. Slots in a metal sheet behave as band-pass filters while unconnected metal elements act as band-stop filters [1]. The theory, analysis and design of FSS were described in [2] and [3]. In recent studies [4] and [5], the FSS structure was used as the resonator device in the waveguide for dielectric permittivity measurements. Moreover, a concept of the CFSS was first introduced in [6] as a hybrid of two closely coupled FSS in which a layer of conducting elements and a layer of aperture elements are etched either side of a thin dielectric substrate. The schematic representation of CFSS structure is shown in Figure 1. The CFSS structure is advantageous compared to conventional FSS structure due to having a highly stable passband with angle of incidence [6], [7] and being miniaturised due to the extra capacitance [8]. Additional CFSS studies were also conducted in [9]–[11].

As a result of studies [8], [11], the CFSS structure has the potential capability to be used for dielectric property measurements by observing the shift in resonant frequency. Therefore, an accurate and precise determination of the measured resonant frequency becomes critical. In order to accurately measure the change in the measured resonant frequency, the Q factor of the CFSS should be maximised. In this paper, the physical and dielectric parameters of the CFSS structure were studied. Based on this analysis an optimised CFSS structure was designed using real materials.

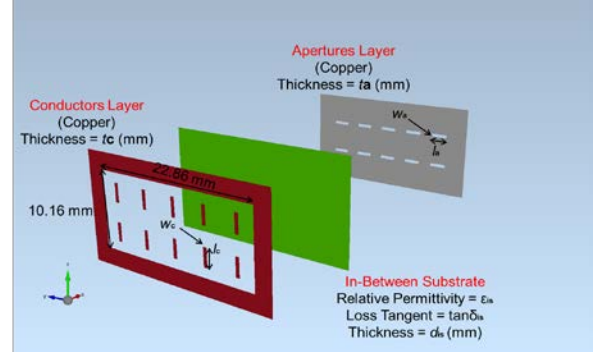


Figure 1: Schematic exploded view of CFSS structure

## 2 Method

The CFSS structure was deployed inside an X-band waveguide. The X-band waveguide frequency range was from 8.2 to 12.4 GHz, and the size was 22.86 mm  $\times$  10.16 mm. The width and height of the CFSS structure were designed to fit in the X-band waveguide and were 22.86 mm and 10.16 mm, respectively. The conductors and the apertures layer were copper. The simulations were conducted using Empire XPU commercial electromagnetic software. In the simulations, unless the designated parameter was studied, the common data used were: conductors length ( $l_c$ ) = 2.5 mm; conductors width ( $w_c$ ) = 0.5 mm; conductors layer thickness ( $t_c$ ) = 0.017 mm; apertures length ( $l_a$ ) = 2.5 mm; apertures width ( $w_a$ ) = 0.5 mm; apertures layer thickness ( $t_a$ ) = 0.017 mm; in-between substrate: relative permittivity ( $\epsilon_s$ ) = 4; loss tangent ( $\tan \delta_s$ ) = 0.01 and thickness ( $d_s$ ) = 0.05 mm. The CFSS consisted of two rows of five conductors and apertures as shown in Figure 1. In the simulations the CFSS was placed inside the waveguide hence the external surface of the waveguide was continuous.

## 3 Parameter Optimisation

The CFSS structure consisted of three parts: conductors layer, in-between substrate and apertures layer. Note, in this section the dimensions of the apertures and conductors were varied independently.

### 3.1 Conductors Layer

The conductors layer are inherently a band-stop filter. When the conductor is larger, the Q factor of the CFSS is higher. Therefore, as either the length or the width of the conductor increased, the Q factor increased. When the conductor length was increased from 2.5 mm to 3.5 mm, the Q factor increased by 13%. Meanwhile, as the width was increased from 0.5 mm to 1.5 mm, the Q factor increased by 3%. The thickness of the conductors layer was also considered and the result show the Q factor slightly decreased when the thickness increased. The three parameter results for the conductors layer are shown in Figure 2.

### 3.2 Apertures Layer

In contrast to the conductors layer, the apertures layer acts as a band-pass filter. When the aperture was larger, the Q factor of the CFSS was reduced. As the length or the width of the aperture was increased, the Q factor decreased as expected. When the length increased from 2.5 mm to 3.5 mm, the Q factor decreased by 38%. The Q factor decreased by 46% when the width increased from 0.5 mm to 1.5 mm. The Q factor slightly increased when the thickness of the apertures layer increased. The three parameter results for the apertures layer are shown in Figure 3. Therefore, a higher Q factor CFSS can be designed when the apertures are shorter and narrower.

### 3.3 In-Between Substrate

The properties and thickness of the in-between substrate were considered as the parameters affecting the Q factor. A higher Q factor was found when the coupling between the conductors and apertures layers was stronger. As shown in Figure 4, a higher relative permittivity, lower loss tangent and thinner thickness of the in-between substrate produced a higher Q factor for the CFSS.

### 3.4 Periodicity

The periodicity of the conductors and apertures is another parameter that affects the Q factor. In Section 3.1, the Q factor increased by 13% when the conductors length was increased from 2.5 mm to 3.5 mm and by 3% when the width was increased from 0.5 mm to 1.5 mm. In Section 3.2, the Q factor decreased by 38% when the conductors length was increased from 2.5 mm to 3.5 mm and by 46% when the width was increased from 0.5 mm to 1.5 mm. It was found that the Q factor was more strongly dependent on the apertures dimensions than the conductors dimensions. The simulated results of different number of rows of conductors/apertures are shown in Figure 5. The Q factor, as expected, decreased when there were more rows of the conductors/apertures. As a result, it is preferred to have fewer rows of the conductors/apertures in the CFSS structure to achieve a higher Q factor.

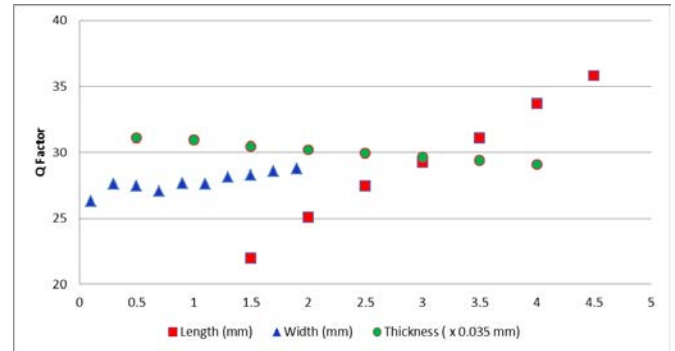


Figure 2: Variation of Q factor with change in conductor length, width and thickness

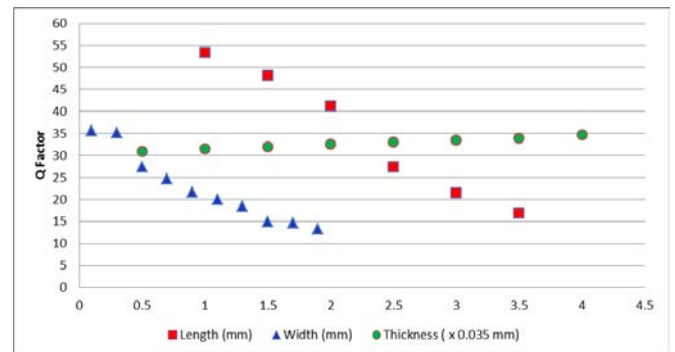


Figure 3: Variation of Q factor with change in aperture length, width and thickness

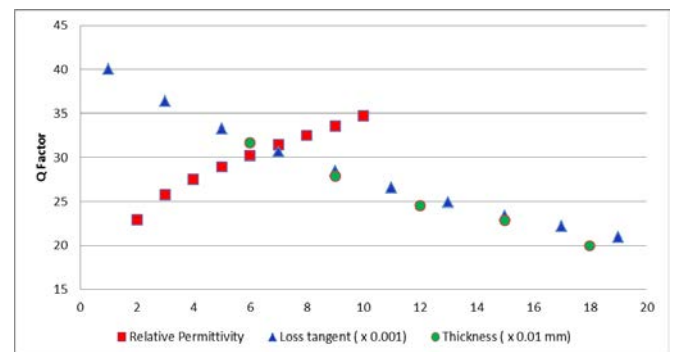


Figure 4: Variation of Q factor with change in in-between substrate relative permittivity, loss tangent and thickness

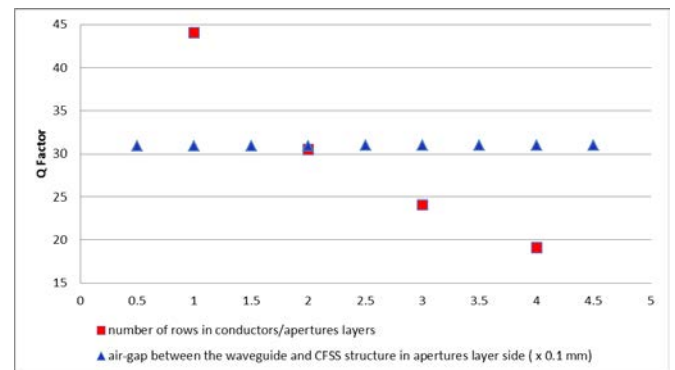


Figure 5: Variation of Q factor with change in number of rows of conductors/apertures layers and the air-gap between the waveguide halves

### 3.5 Air-Gap Between Waveguide Halves

Another possible factor that could affect the Q factor was the air-gap between the waveguide halves. However, from the simulation results shown in Figure 5, the Q factor was not affected when the air-gap existed. The leaking caused by air-gap increased the insertion loss, but did not affect the resonant frequency or the Q factor.

The considered parameters and effects for Q factor are summarized in Table 1. It can be observed that to obtain the highest Q factor, the conductors should be longer; the apertures should be shorter and narrower; the in-between substrate should be thinner, be low loss and have a high relative permittivity; the periodicity should be larger with fewer rows of conductors/apertures.

Table 1: Summary of parameter effects on the Q factor

Parameter		Range	Q factor effect when parameter increased
Conductor	Length (mm)	1.5 to 4.5	Increase
	Width (mm)	0.1 to 1.9	Slightly Decrease (Negligible effect)
	Thickness (mm)	0.0175 to 0.14	Slightly Increase (Negligible effect)
Aperture	Length (mm)	1 to 3.5	Decrease
	Width (mm)	0.1 to 1.9	Decrease
	Thickness (mm)	0.0175 to 0.14	Slightly Increase (Negligible effect)
In-Between Substrate	Relative Permittivity	2 to 10	Increase
	Loss Tangent	0.001 to 0.019	Decrease
	Thickness (mm)	0.06 to 0.18	Decrease
Periodicity	Number of Rows	1 to 4	Decrease
Air-Gap	Air-Gap (mm)	0.05 to 0.45	No Effect

## 4 CFSS Measurements

A CFSS was designed and fabricated using material Rogers XT/duroid 8100 as shown in Figure 6. The data were: conductors length ( $l_c$ ) = 5 mm; conductors width ( $w_c$ ) = 0.5 mm; conductors layer thickness ( $t_c$ ) = 0.017 mm; apertures length ( $l_a$ ) = 2.5 mm; apertures width ( $w_a$ ) = 0.5 mm; apertures layer thickness ( $t_a$ ) = 0.017 mm; in-between substrate: relative permittivity ( $\epsilon_{is}$ ) = 3.54; loss tangent ( $\tan\delta_{is}$ ) = 0.0049 and thickness ( $d_{is}$ ) = 0.05 mm. The CFSS consisted of one row of five conductors/apertures. The simulation results were compared to the measurements using two different VNA systems and demonstrated a very good agreement as shown in Figure 7.

## 5 Conclusion

The effect of the physical and dielectric parameters in the CFSS structure for a higher Q factor has been studied and presented in this paper. A CFSS sample was designed and fabricated. The measurement results of the sample from two different VNA systems have also shown a very good agreement with the simulations which highlights the repeatability of the measurements. Future work will consider potential capability of the CFSS in a waveguide to be used for dielectric property measurements.

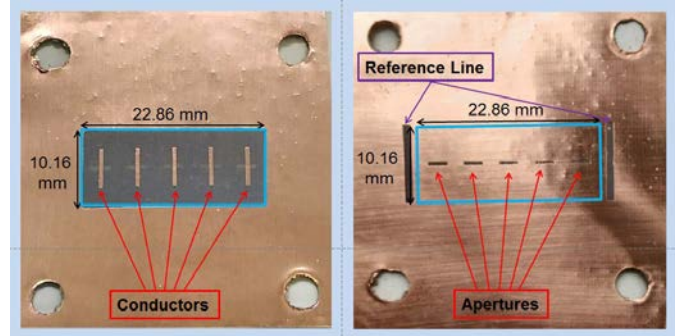


Figure 6: Front and back views of the CFSS

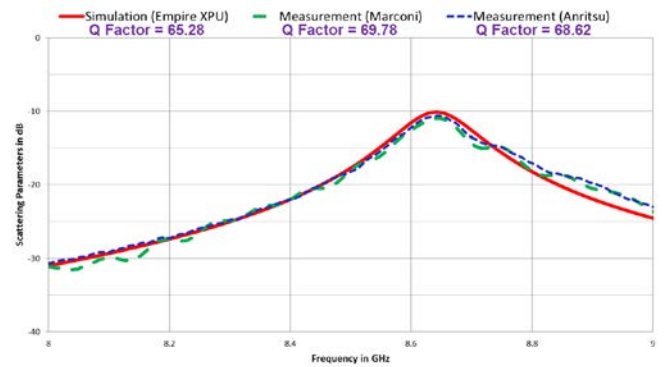


Figure 7: Measured and simulated  $S_{21}$  and Q factor of the CFSS

## References

- [1] J. D. Ortiz, J. D. Baena, V. Losada, F. Medina, R. Marqués, and J. L. A. Quijano, "Self-complementary metasurface for designing narrow band pass/stop filters," *IEEE Microw. Wirel. Components Lett.*, vol. 23, no. 6, pp. 291–293, 2013.
- [2] J. C. Vardaxoglou, *Frequency Selective Surfaces: Analysis and Design*. Research Studies Press, 1997.
- [3] B. A. Munk, *Frequency Selective Surfaces: Theory and Design*. New York: John Wiley&Sons, Inc., 2000.
- [4] F. Costa, C. Amabile, A. Monorchio, and E. Prati, "Waveguide dielectric permittivity measurement technique based on resonant FSS filters," *IEEE Microw. Wirel. Components Lett.*, vol. 21, no. 5, pp. 273–275, 2011.
- [5] F. Costa, A. Monorchio, C. Amabile, and E. Prati, "Dielectric permittivity measurement technique based on waveguide FSS filters," *41st Eur. Microw. Conf.*, vol. 21, no. October, pp. 945–948, 2011.
- [6] D.S.Lockyer, J.C.Vardaxoglou, and R.A.Simpkin, "Complementary frequency selective surfaces," *IEE Proc -Microw Antennas Propag*, vol. 147, no. 6, pp. 501–507, 2000.
- [7] L. Zheng, S. Qu, J. Zhang, J. Wang, M. Yang, Y. Li, H. Zhou, and A. Zhang, "Fabrication of dual-passband frequency selective surface utilizing complementary structure," *2015 IEEE MTT-S Int. Microw. Work. Ser. Adv. Mater. Process. RF THz Appl. IEEE MTT-S IMWS-AMP 2015 - Proc.*, pp. 3–

- 5, 2015.
- [8] C. C. Njoku, "A study on the properties of complementary frequency selective surfaces for dielectric measurements," *Loughbrgh. Antennas Propag. Conf.*, pp. 15–18, 2015.
- [9] S. S. Bukhari, W. G. Whittow, J. C. Vardaxoglou, and S. Maci, "Square loop complementary frequency selective surfaces," *IEEE Antennas Propag. Soc. AP-S Int. Symp.*, pp. 1258–1259, 2015.
- [10] S. S. Bukhari, W. G. Whittow, J. C. Vardaxoglou, and S. Maci, "Dipole loaded complementary Frequency Selective Surfaces," *2015 Usn. Radio Sci. Meet. (Joint with AP-S Symp. Usn. 2015 - Proc.)*, p. 97, 2015.
- [11] C. C. Njoku, J. C. Vardaxoglou, and W. G. Whittow, "Complementary frequency selective surfaces in a waveguide simulator," *7th Eur. Conf. Antennas Propag.*, no. 1, pp. 2420–2422, 2013.